Dual Receptor-Targeting Tc-99m-Labeled Arg-Gly-Asp-Conjugated Alpha-Melanocyte Stimulating Hormone Hybrid Peptides for Human Melanoma Imaging

Jingli Xu[1], **Jianquan Yang**[1], and **Yubin Miao**[1,2,3]

[1]College of Pharmacy, University of New Mexico, Albuquerque, NM 87131, USA

[2]Cancer Research and Treatment Center, University of New Mexico, Albuquerque, NM 87131, USA

[3]Department of Dermatology, University of New Mexico, Albuquerque, NM 87131, USA

Abstract

Introduction—The aim of this study was to examine whether the substitution of the Lys linker with the aminooctanoic acid (Aoc) and polyethylene glycol (PEG) linker could substantially decrease the non-specific renal uptake of ^{99m}Tc-labeled Arg-Gly-Asp-conjugated α-melanocyte stimulating hormone (α-MSH) hybrid peptides.

Methods—The RGD motif {Arg-Gly-Asp-DTyr-Asp} was coupled to [Cys^{3,4,10}, D-Phe^7, Arg^{11}]α-MSH$_{3–13}$ via the Aoc or PEG$_2$ linker to generate RGD-Aoc-(Arg^{11})CCMSH and RGD-PEG-(Arg^{11})CCMSH. The biodistribution results of ^{99m}Tc-RGD-Aoc-(Arg^{11})CCMSH and ^{99m}Tc-RGD-PEG$_2$-(Arg^{11})CCMSH were examined in M21 human melanoma-xenografted nude mice.

Results—The substitution of Lys linker with Aoc and PEG$_2$ linker significantly reduced the renal uptake of ^{99m}Tc-RGD-Aoc-(Arg^{11})CCMSH and ^{99m}Tc-RGD-PEG$_2$-(Arg^{11})CCMSH by 58% and 63% at 2 h post-injection. The renal uptake of ^{99m}Tc-RGD-Aoc-(Arg^{11})CCMSH and ^{99m}Tc-RGD-PEG$_2$-(Arg^{11})CCMSH was 27.93 ± 3.98 and 22.01 ± 9.89% ID/g at 2 h post-injection. ^{99m}Tc-RGD-Aoc-(Arg^{11})CCMSH displayed higher tumor uptake than ^{99m}Tc-RGD-PEG$_2$-(Arg^{11})CCMSH (2.35 ± 0.12 vs. 1.71 ± 0.25% ID/g at 2 h post-injection). The M21 human melanoma lesions could be clearly visualized by SPECT/CT using ^{99m}Tc-RGD-Aoc-(Arg^{11})CCMSH as an imaging probe.

Conclusions—The favorable effect of Aoc and PEG$_2$ linker in reducing the renal uptake provided a new insight into the design of novel dual receptor-targeting radiolabeled peptides.

Corresponding Author: Yubin Miao, 2502 Marble NE, MSC09 5360, College of Pharmacy, University of New Mexico, Albuquerque, NM 87131-0001. Phone: (505) 925-4437; Fax: (505) 272-6749; ymiao@salud.unm.edu.

Keywords

Arg-Gly-Asp-conjugated; alpha-melanocyte stimulating hormone hybrid peptide; dual receptor-targeting human melanoma imaging

INTRODUCTION

Over the past decade, both radiolabeled alpha-melanocyte stimulating hormone (α-MSH) peptides and Arg-Gly-Asp (RGD) peptides have been reported for receptor-targeting melanoma imaging [1–16]. Specifically, the radiolabeled α-MSH peptides have been utilized to target melanocortin-1 (MC1) receptors [1–11], whereas the radiolabeled RGD peptides have been employed to target $\alpha_v\beta_3$ integrin receptors [12–16]. In consideration of the expressions of MC1 and $\alpha_v\beta_3$ integrin receptors on human melanoma cells, we developed a RGD-conjugated α-MSH hybrid peptide which could target both MC1 and $\alpha_v\beta_3$ integrin receptors for melanoma detection [17]. We demonstrated that the unique dual receptor-targeting ^{99m}Tc-RGD-Lys-(Arg^{11})CCMSH {cyclic(Arg-Gly-Asp-DTyr-Asp)-Lys-(^{99m}Tc-[Cys^{3,4,10}, D-Phe^7, Arg^{11}]α-MSH$_{3–13}$)} hybrid peptide displayed significantly higher tumor uptake than ^{99m}Tc-labeled α-MSH or RGD peptide targeting only the MC1 or $\alpha_v\beta_3$ integrin receptor [17]. Flank M21 human melanoma-xenografted tumors were clearly visualized by SPECT/CT using ^{99m}Tc-RGD-Lys-(Arg^{11})CCMSH as an imaging probe [17].

Despite the success of ^{99m}Tc-RGD-Lys-(Arg^{11})CCMSH for human melanoma imaging, ^{99m}Tc-RGD-Lys-(Arg^{11})CCMSH displayed extremely high non-specific renal uptake of 90.80 ± 19.35% ID/g at 4 h post-injection in M21 human melanoma-xenografted nude mice [17]. It is desirable to decrease the renal uptake to facilitate the potential therapeutic application when labeling the peptide with therapeutic ^{188}Re/^{186}Re (β-emitters). Interestingly, the co-injection of L-Lysine reduced the renal uptake of ^{99m}Tc-RGD-Lys-(Arg^{11})CCMSH by 52% at 2 h post-injection without affecting the tumor uptake [18], suggesting that the overall positive charge of ^{99m}Tc-RGD-Lys-(Arg^{11})CCMSH substantially contributed to its non-specific renal uptake. Thus, we hypothesized that the reduction of the overall positive charge of ^{99m}Tc-RGD-Lys-(Arg^{11})CCMSH would decrease the non-specific renal uptake. Clearly, three Arg residues and one Lys linker represent the positive charges of ^{99m}Tc-RGD-Lys-(Arg^{11})CCMSH. However, three Arg residues are critical to the MC1 or $\alpha_v\beta_3$ integrin receptor binding. Thus, we substituted the positively-charged Lys linker with neutral aminooctanoic acid (Aoc) and polyethylene glycol (PEG) linker to decrease the overall positive charge of the peptide to determine whether such change could substantially reduce the non-specific renal uptake.

We synthesized two new RGD-conjugated α-MSH hybrid peptides with the Aoc and PEG$_2$ linkers. Specifically, the RGD motif {Arg-Gly-Asp-DTyr-Asp} was coupled to [Cys^{3,4,10}, D-Phe^7, Arg^{11}]α-MSH$_{3–13}$ peptide via the Aoc or PEG$_2$ linker to generate RGD-Aoc-(Arg^{11})CCMSH and RGD-PEG-(Arg^{11})CCMSH. We determined their receptor binding affinities in M21 human melanoma cells. Then, we radiolabeled RGD-Aoc-(Arg^{11})CCMSH and RGD-PEG$_2$-(Arg^{11})CCMSH with ^{99m}Tc and examine their tumor targeting and biodistribution properties in M21 human melanoma-xenografted nude mice.

EXPERIMENTAL PROCEDURES

Chemicals and reagents

Amino acid and resin were purchased from Advanced ChemTech (Louisville, KY, USA) and Novabiochem (San Diego, CA, USA). $^{99m}TcO_4^-$ was purchased from Cardinal Health (Albuquerque, NM). ^{125}I-Tyr^2-(Nle^4, $_D$Phe^7)-α-MSH [^{125}I-(Tyr^2)-NDP-MSH] and ^{125}I-Echistatin were obtained from PerkinElmer (Shelton, CT, USA) for competitive receptor binding assay. All other chemicals used in this study were purchased from Thermo Fisher Scientific (Waltham, MA, USA) and used without further purification. The M21 human melanoma cells were supplied by Dr. David A. Cheresh from the Department of Pathology, Moores University of California-San Diego Cancer Center.

Peptide Synthesis

RGD-Aoc-(Arg^{11})CCMSH and RGD-PEG$_2$-(Arg^{11})CCMSH were synthesized using fluorenylmethyloxy carbonyl (Fmoc) chemistry, purified by reverse phase-high performance liquid chromatography (RP-HPLC) and characterized by liquid chromatography-mass spectrometry (LC-MS). Basically, 70 μmol of resin and 210 μmol of each Fmoc-protected amino acid were used for the synthesis. Briefly, the intermediate scaffolds of H$_2$N-Arg(Pbf)-Ala-Asp(OtBu)-$_D$Tyr(tBu)-Asp(O-2-phenylisopropyl)-Aoc/PEG$_2$-Cys(Trt)-Cys(Trt)-Glu(OtBu)-His(Trt)-$_D$Phe-Arg(Pbf)-Trp(Boc)-Cys(Trt)-Arg(Pbf)-Pro-Val were synthesized on H$_2$N-Sieber amide resin by an Advanced ChemTech multiple-peptide synthesizer (Louisville, KY). The protecting groups of 2-phenylisopropyl were removed and the peptides were cleaved from the resin treating with a mixture of 2.5% of trifluoroacetic acid (TFA) and 5% of triisopropylsilane. After the precipitation with ice-cold ether and characterization by LC-MS, the protected peptides were dissolved in H$_2$O/CH$_3$CN (50:50) and lyophilized to remove the reagents such as TFA and triisopropylsilane. The protected peptides were further cyclized by coupling the carboxylic group from the Asp with the alpha amino group from the Arg at the N-terminus. The cyclization reaction was achieved by overnight reaction in dimethylformamide (DMF) using benzotriazole-1-*yl-oxy-tris*-pyrrolidino-phosphonium-hexafluorophosphate (PyBOP) as a coupling agent in the presence of *N,N*-diisopropylethylamine (DIEA). After characterization by LC-MS, the cyclized protected peptides were dissolved in H$_2$O/CH$_3$CN (50:50) and lyophilized to remove the reagents. The protecting groups were totally removed by treating with a mixture of trifluoroacetic acid (TFA), thioanisole, phenol, water, ethanedithiol and triisopropylsilane (87.5:2.5:2.5:2.5:2.5:2.5) for 2 h at room temperature (25 °C). The peptides were precipitated and washed with ice-cold ether for four times, purified by RP-HPLC and characterized by LC-MS.

In vitro competitive binding assay

The IC$_{50}$ values of RGD-Aoc-(Arg^{11})CCMSH and RGD-PEG$_2$-(Arg^{11})CCMSH peptides were determined in M21 human melanoma cells. The receptor binding assay was replicated in triplicate for each peptide. ^{125}I-(Tyr^2)-NDP-MSH and ^{125}I-Echistatin were used as radioligands for MC1 and $\alpha_v\beta_3$ integrin receptors, respectively. For MC1 receptor binding assay, the M21 cells (1.5×10^5 cells/well, n=3) were incubated at 37 °C for 2 h with approximately 30,000 counts per minute (cpm) of ^{125}I-(Tyr^2)-NDP-MSH in the presence of

10^{-12} to 10^{-5} M of each peptide in 0.3 mL of binding medium {Modified Eagle's medium with 25 mM N-(2-hydroxyethyl)-piperazine-N'-(2-ethanesulfonic acid), pH 7.4, 0.2% bovine serum albumin (BSA), 0.3 mM 1,10-phenathroline}. The binding medium was aspirated after the incubation. The cells were rinsed twice with 0.5 ml of ice-cold pH 7.4, 0.2% BSA/0.01 M phosphate buffered saline (PBS) and lysed in 0.5 mL of 1 N NaOH for 5 min. The cells were harvested and measured in a Wallac 1480 automated gamma counter (PerkinElmer, NJ). The IC_{50} values of the peptides for the MC1 receptor were calculated using the Prism software (GraphPad Software, La Jolla, CA, USA).

For $\alpha_v\beta_3$ integrin receptor binding assay, the M21 cells (1×10^5 cells/well, n=3) were seeded in Millipore 96-well filter multiscreen DV plates (0.65 µm pore size) and incubated at 25 °C for 2 h with approximately 30,000 counts per minute (cpm) of ^{125}I-Echistatin in the presence of 10^{-11} to 10^{-4} M of each peptide in 0.2 mL of binding medium. After the incubation, the plates were filtered through a multiscreen vacuum manifold and rinsed twice with 0.5 ml of ice-cold pH 7.4, 0.2% BSA/0.01 M PBS. The hydrophilic polyvinylidenedifluoride filters were collected and counted in a Wallac 1480 automated gamma counter. The IC_{50} values of the peptides for the $\alpha_v\beta_3$ integrin receptor were calculated using the Prism software.

Peptide radiolabeling

RGD-Aoc-(Arg^{11})CCMSH and RGD-PEG$_2$-(Arg^{11})CCMSH peptides were labeled with ^{99m}Tc via a direct reduction reaction using SnCl$_2$. Briefly, 10 µL of 1 mg/mL SnCl$_2$ in 0.1 M HCl, 40 µL of 0.5 M NH$_4$OAc (pH 5.2), 100 µL of 0.2 M Na$_2$tartate (pH 9.2), 100 µL of fresh ^{99m}TcO$_4^-$ solution (37–74 MBq), and 10 µL of 1 mg/mL of each peptide in aqueous solution were added into a reaction vial and incubated at 25 °C for 20 min to form ^{99m}Tc-labeled peptide. Each ^{99m}Tc-peptide was purified to a single species by Waters RP-HPLC (Milford, MA) on a Grace Vydac C-18 reverse phase analytic column (Deerfield, IL) using a 20-min gradient of 16–26% acetonitrile in 20 mM HCl aqueous solution at a flow rate of 1 mL/min. Each purified peptide was purged with N$_2$ gas for 20 min to remove the acetonitrile. The pH of final peptide solution was adjusted to 7.4 with 0.1 N NaOH and sterile normal saline for animal studies.

Biodistribution studies

All the animal studies were conducted in compliance with Institutional Animal Care and Use Committee approval. The biodistribution of ^{99m}Tc-RGD-Aoc-(Arg^{11})CCMSH was determined in M21 melanoma-xenografted nude mice (Harlan, Indianapolis, IN). Each nude mouse was subcutaneously inoculated with 5×10^6 M21 human melanoma cells on the right flank. The weight of tumors reached approximately 0.1–0.2 g 21 days post cell inoculation. Each melanoma-xenografted nude mouse was injected with 0.037 MBq of ^{99m}Tc-RGD-Aoc-(Arg^{11})CCMSH via the tail vein. Groups of 5 mice were sacrificed at 0.5, 2, 4 and 24 h post-injection, and tumors and organs of interest were harvested, weighed and counted. The receptor specificity of the tumor uptake was determined by co-injecting ^{99m}Tc-RGD-Aoc-(Arg^{11})CCMSH with unlabeled RGD-Aoc-(Arg^{11})CCMSH. Each melanoma-xenografted nude mouse was injected with 0.037 MBq of ^{99m}Tc-RGD-Aoc-(Arg^{11})CCMSH with 6.1 nmol of unlabeled RGD-Aoc-(Arg^{11})CCMSH via the tail vein. A group of 5 mice were

sacrificed at 2 h post-injection, and tumors and organs of interest were harvested, weighed and counted. Blood values were taken as 6.5% of the whole-body weight. The biodistribution of ^{99m}Tc-RGD-PEG$_2$-(Arg^{11})CCMSH was only determined in M21 melanoma-xenografted nude mice at 2 h post-injection for comparison.

Imaging human melanoma with ^{99m}Tc-RGD-Aoc-(Arg^{11})CCMSH

We determined the melanoma imaging property of ^{99m}Tc-RGD-Aoc-(Arg^{11})CCMSH. Approximately 9.2 MBq of ^{99m}Tc-RGD-Aoc-(Arg^{11})CCMSH was injected into a M21 human melanoma-xenografted nude mouse via the tail vein. The mouse was euthanized for small animal SPECT/CT (Nano-SPECT/CT$^®$, Bioscan, Washington DC) imaging at 2 h post-injection. The 9-min CT imaging was immediately followed by the SPECT imaging of whole-body. The SPECT scans of 24 projections were acquired. Reconstructed data from SPECT and CT were visualized and co-registered using InVivoScope (Bioscan, Washington DC).

Statistical methods

Statistical analysis was performed using the Student's t-test for unpaired data to determine the significant differences between the groups in the biodistribution and peptide blocking studies described above. Differences at the 95% confidence level ($p < 0.05$) were considered significant.

RESULTS

The schematic structures of RGD-Aoc-(Arg^{11})CCMSH and RGD-PEG$_2$-(Arg^{11})CCMSH are shown in Figure 1. RGD-Aoc-(Arg^{11})CCMSH and RGD-PEG$_2$-(Arg^{11})CCMSH were synthesized and purified by RP-HPLC. The overall synthetic yields were approximately 28–30% for RGD-Aoc-(Arg^{11})CCMSH and RGD-PEG$_2$-(Arg^{11})CCMSH. Both peptides displayed greater than 95% purity after HPLC purification. The identities of RGD-Aoc-(Arg^{11})CCMSH and RGDPEG$_2$-(Arg^{11})CCMSH were confirmed by mass spectrometry. The found molecular weights matched the calculated molecular weights. The competitive binding curves of the peptides for MC1 and $\alpha_v\beta_3$ integrin receptors are presented in Figure 2. The IC$_{50}$ values of RGD-Aoc-(Arg^{11})CCMSH and RGD-PEG$_2$-(Arg^{11})CCMSH were 1.5 ± 0.2 and 1.9 ± 0.2 nM for the MC1 receptor. The IC$_{50}$ values of RGD-Aoc-(Arg^{11})CCMSH and RGD-PEG$_2$-(Arg^{11})CCMSH were 1125 ± 26 and 1479 ± 74 nM for the $\alpha_v\beta_3$ integrin receptor. RGD-Aoc-(Arg^{11})CCMSH and RGD-PEG$_2$-(Arg^{11})CCMSH were easily labeled with ^{99m}Tc with greater than 95% radiolabeling yields. ^{99m}Tc-RGD-Aoc-(Arg^{11})CCMSH and ^{99m}Tc-RGD-PEG$_2$-(Arg^{11})CCMSH showed greater than 98% radiochemical purities after the HPLC purification. ^{99m}Tc-RGD-Aoc-(Arg^{11})CCMSH and ^{99m}Tc-RGD-PEG$_2$-(Arg^{11})CCMSH were completely separated from their excess non-labeled peptides by RP-HPLC. The specific activities of ^{99m}Tc-RGD-Aoc-(Arg^{11})CCMSH and ^{99m}Tc-RGD-PEG$_2$-(Arg^{11})CCMSH were 1.9259×10^{13} and 1.9259×10^{13} MBq/mol, respectively. The retention times of ^{99m}Tc-RGD-Aoc-(Arg^{11})CCMSH and ^{99m}Tc-RGD-PEG$_2$-(Arg^{11})CCMSH were 20.5 and 14.1 min, respectively.

RGD-Aoc-(Arg[11])CCMSH displayed stronger receptor binding affinity than RGD-PEG$_2$-(Arg[11])CCMSH in M21 cells. Thus, the melanoma targeting and biodistribution properties of ^{99m}Tc-RGD-Aoc-(Arg[11])CCMSH were determined in M21 melanoma-xenografted nude mice at 0.5, 2, 4 and 24 h post-injection. The melanoma targeting property of ^{99m}Tc-RGD-PEG$_2$-(Arg[11])CCMSH was determined in M21 melanoma-xenografted nude mice at 2 h post-injection only for comparison. The biodistribution results are shown in Table 1. ^{99m}Tc-RGD-Aoc-(Arg[11])CCMSH exhibited rapid tumor uptake in M21 melanoma-xenografted nude mice. The tumor uptake was 2.42 ± 0.23% ID/g at 0.5 h post-injection. There were 2.35 ± 0.12 and 1.56 ± 0.26% ID/g of the ^{99m}Tc-RGD-Aoc-(Arg[11])CCMSH activity remaining in the tumors 2 and 4 h post-injection. At 24 h post-injection, the tumor uptake was 0.64 ± 0.31% ID/g. Co-injection of unlabeled RGD-Aoc-(Arg[11])CCMSH blocked the tumor uptake by 50% (p<0.05), demonstrating that the tumor uptake was receptor-mediated. Whole-body clearance of ^{99m}Tc-RGD-Aoc-(Arg[11])CCMSH was rapid, with approximately 60% of the injected radioactivity cleared through the urinary system by 2 h post-injection (Table 1). The accumulation of ^{99m}Tc-RGD-Aoc-(Arg[11])CCMSH in normal organs was lower than 5% ID/g except for the kidneys after 2 h post-injection. The renal uptake of ^{99m}Tc-RGD-Aoc-(Arg[11])CCMSH reached its highest value of 37.05 ± 1.76% ID/g at 4 h post-injection and decreased to 14.32 ± 2.37% ID/g at 24 h post-injection. Co-injection of unlabeled RGD-Aoc-(Arg[11])CCMSH did not affect the renal uptake, indicating that the renal uptake was non-specific. ^{99m}Tc-RGD-PEG$_2$-(Arg[11])CCMSH exhibited significantly (p<0.05) lower tumor uptake than that of ^{99m}Tc-RGD-Aoc-(Arg[11])CCMSH. However, the renal uptake was similar between ^{99m}Tc-RGD-Aoc-(Arg[11])CCMSH and ^{99m}Tc-RGD-PEG$_2$-(Arg[11])CCMSH at 2 h post-injection. The melanoma imaging property of ^{99m}Tc-RGD-Aoc-(Arg[11])CCMSH was examined in M21 human melanoma-xenografted nude mice (Figure 3). Flank M21 human melanoma tumors were visualized clearly by ^{99m}Tc-RGD-Aoc-(Arg[11])CCMSH at 2 h post-injection.

DISCUSSION

We are interested in developing novel hybrid peptides to target both MC1 and $\alpha_v\beta_3$ integrin receptors for melanoma imaging because both receptors are over-expressed on melanoma cells. For instance, the receptor densities of MC1 and $\alpha_v\beta_3$ integrin receptors were 1,281 and 96,555 receptors/cell on M21 human melanoma cells [17]. In the mean time, several potential advantages are associated with dual receptor-targeting hybrid peptide as compared to single receptor-targeting peptide. Firstly, the overall receptor density increases for the dual receptor-targeting hybrid peptide because it can target both MC1 and $\alpha_v\beta_3$ integrin receptors. Thus, targeting dual receptors will capture a larger audience of MC1 and $\alpha_v\beta_3$ integrin receptor-expressing melanoma lesions. Secondly, a potential synergistic effect between the MC1 and $\alpha_v\beta_3$ integrin receptors could facilitate the binding of the hybrid peptides to receptors by elevating the regional peptide concentration in the proximity of receptors. For instance, the hybrid peptide bound to either MC1 or $\alpha_v\beta_3$ integrin receptor would be in the close proximity of other available receptors. When the hybrid peptide dissociates from the current receptor, it has more opportunities to bind to other receptors in the close proximity. In our previous report [17], ^{99m}Tc-RGD-Lys-(Arg[11])CCMSH showed higher M21 melanoma uptake than ^{99m}Tc-RAD-Lys-(Arg[11])CCMSH or ^{99m}Tc-RGD-Lys-

(Arg[11])CCMSH$_{scramble}$. The melanoma uptake of ^{99m}Tc-RGD-Lys-(Arg[11])CCMSH was 2.5 and 2.2 times the tumor uptake of ^{99m}Tc-RAD-Lys-(Arg[11])CCMSH and ^{99m}Tc-RGD-Lys-(Arg[11])CCMSH$_{scramble}$, respectively.

One potential application of the dual receptor-targeting hybrid peptide is to label it with therapeutic radionuclides such as ^{188}Re or ^{186}Re. Both ^{99m}Tc and ^{188}Re/^{186}Re share similar coordination chemistry. It is worthwhile to note that the (Arg[11])CCMSH motif not only serves as a MC1 receptor binding moiety, but also serves as a site-specific chelating system for direct labeling of ^{99m}Tc/^{188}Re/^{186}Re. Specifically, three -SH groups from Cys^3, Cys^4 and Cys^{10} and one -NH from Cys^4 yield a NS$_3$ chelating system for ^{99m}Tc/^{188}Re/^{186}Re. In other words, the radiolabeling and peptide cyclization can be accomplished simultaneously during the radiolabeling process. Meanwhile, the conjugation of Tc and Re metals to the (Arg[11])CCMSH motif didn't affect the MC1 receptor binding. Both linear (Arg[11])CCMSH and cyclized Re-(Arg[11])CCMSH peptides exhibited similar MC1 receptor binding affinities (1.7 vs. 1.9 nM, respectively) [22].

Despite the success of ^{99m}Tc-RGD-Lys-(Arg[11])CCMSH for human melanoma imaging, ^{99m}Tc-RGD-Lys-(Arg[11])CCMSH displayed extremely high renal uptake (90.80 ± 19.35% ID/g at 4 h post-injection) in M21 human melanoma-xenografted nude mice [17]. Thus, it is necessary to reduce the non-specific renal uptake to facilitate the potential therapeutic application. In this study, we substituted the Lys linker with Aoc or PEG$_2$ linker to examine whether the linker change could substantially reduce the renal uptake. The substitution of the Lys linker with Aoc or PEG$_2$ linker retained low nanomolar MC1 receptor binding affinity (1.5–1.9 nM), but decreased the $\alpha_v\beta_3$ integrin receptor binding affinity by 2- to 3-fold. It was likely that the longer hydrocarbon chains from Aoc and PEG$_2$ linker somehow affected the $\alpha_v\beta_3$ integrin receptor binding. Despite that the length of Aoc linker is as same as the length of PEG$_2$ linker, RGD-Aoc-(Arg[11])CCMSH displayed slightly stronger binding affinities to both MC1 and $\alpha_v\beta_3$ integrin receptor than RGD-PEG$_2$-(Arg[11])CCMSH. Thus, we fully determined the melanoma targeting and imaging properties of ^{99m}Tc-RGD-Aoc-(Arg[11])CCMSH while we only examined the biodistribution property of ^{99m}Tc-RGD-PEG$_2$-(Arg[11])CCMSH at 2 h post-injection for comparison.

The biodistribution results of ^{99m}Tc-RGD-Aoc-(Arg[11])CCMSH and ^{99m}Tc-RGD-PEG$_2$-(Arg[11])CCMSH in M21 human melanoma xenografts supported our hypothesis. The substitution of the Lys linker with the Aoc and PEG$_2$ linker substantially decreased the renal uptake (Figure 4). The kidney uptake of ^{99m}Tc-RGD-Aoc-(Arg[11])CCMSH was 31%, 42%, 41% and 51% of the kidney uptake of ^{99m}Tc-RGD-Lys-(Arg[11])CCMSH at 0.5, 2, 4 and 24 h post-injection respectively. Meanwhile, the tumor uptake of ^{99m}Tc-RGD-Aoc-(Arg[11])CCMSH was comparable as the tumor uptake of ^{99m}Tc-RGD-Lys-(Arg[11])CCMSH at 0.5 and 2 h post-injection. It is worthwhile to note that the co-injection of 6.1 nmol (~13 µg) of peptide blockade decreased the tumor uptake of ^{99m}Tc-RGD-Aoc-(Arg[11])CCMSH by 50%. Generally, approximately 200–300 µg of RGD peptide are used for tumor blocking studies. Thus, it was likely that greater than 6.1 nmol (~13 µg) of peptide blockade would be needed to further block the tumor uptake of ^{99m}Tc-RGD-Aoc-(Arg[11])CCMSH. Although ^{99m}Tc-RGD-PEG$_2$-(Arg[11])CCMSH exhibited similar renal uptake as ^{99m}Tc-RGD-Aoc-(Arg[11])CCMSH, the tumor uptake of ^{99m}Tc-RGD-PEG$_2$-(Arg[11])CCMSH was

significantly ($p<0.05$) lower than that of ^{99m}Tc-RGD-Aoc-(Arg[11])CCMSH at 2 h post-injection. As shown in Figure 3, the M21 human melanoma lesions could be clearly visualized by SPECT/CT using ^{99m}Tc-RGD-Aoc-(Arg[11])CCMSH as an imaging probe.

The receptor binding affinities need to be similar for the dual receptor-targeting peptide to have maximal effect. Despite the success of ^{99m}Tc-RGD-Aoc-(Arg[11])CCMSH in terms of decreased renal uptake, it is worthwhile to note that the binding affinity of RGD-Aoc-(Arg[11])CCMSH for $\alpha_v\beta_3$ integrin receptor was in low micromolar range. Although the $\alpha_v\beta_3$ integrin receptor density is 96,555 receptors/cell on M21 human melanoma cells [17], such receptor density might not be sufficient to overcome the weak $\alpha_v\beta_3$ integrin receptor binding. Thus, it is necessary to improve the receptor binding affinity of the hybrid peptide for $\alpha_v\beta_3$ integrin receptor to enhance the benefit of dual receptor-targeting peptide. One potential way would be the optimization of the linker length between the RGD and (Arg[11])CCMSH moieties. The impact of linker length on receptor binding affinity was reported for bombesin peptides [19–21]. For instance, the DOTA-conjugated bombesin peptides with 5-carbon to 8-carbon hydrocarbon linkers exhibited 0.6–1.7 nM receptor binding affinities, whereas the DOTA-conjugated bombesin peptides with either shorter or longer hydrocarbon linkers displayed much weaker receptor binding by 100-fold. It is worthwhile to note that the substitution of the Lys linker with Aoc linker decreased the $\alpha_v\beta_3$ integrin receptor binding by 2.8-fold in this report. Obviously, the hydrocarbon chain of Aoc is longer than that of Lys. The impact on the $\alpha_v\beta_3$ integrin receptor binding indicated that the longer hydrocarbon chain of Aoc somehow influenced the $\alpha_v\beta_3$ integrin receptor binding. One possible way to restore and improve the $\alpha_v\beta_3$ integrin receptor binding would be replacing the Aoc linker with Gly so that the linker length would be as same as Lys. It would be interesting to examine this hypothesis in the future.

CONCLUSIONS

The substitution of Lys linker with Aoc and PEG$_2$ linker significantly reduced the renal uptake of ^{99m}Tc-RGD-Aoc-(Arg[11])CCMSH and ^{99m}Tc-RGD-PEG$_2$-(Arg[11])CCMSH by 58% and 63% at 2 h post-injection. ^{99m}Tc-RGD-Aoc-(Arg[11])CCMSH displayed higher tumor uptake than ^{99m}Tc-RGD-PEG$_2$-(Arg[11])CCMSH in M21 human melanoma xenografted nude mice. The M21 human melanoma lesions could be clearly visualized by SPECT/CT using ^{99m}Tc-RGD-Aoc-(Arg[11])CCMSH as an imaging probe. The favorable effect of Aoc and PEG$_2$ linker in reducing the renal uptake provided a new insight into the design of novel dual receptor-targeting radiolabeled peptides.
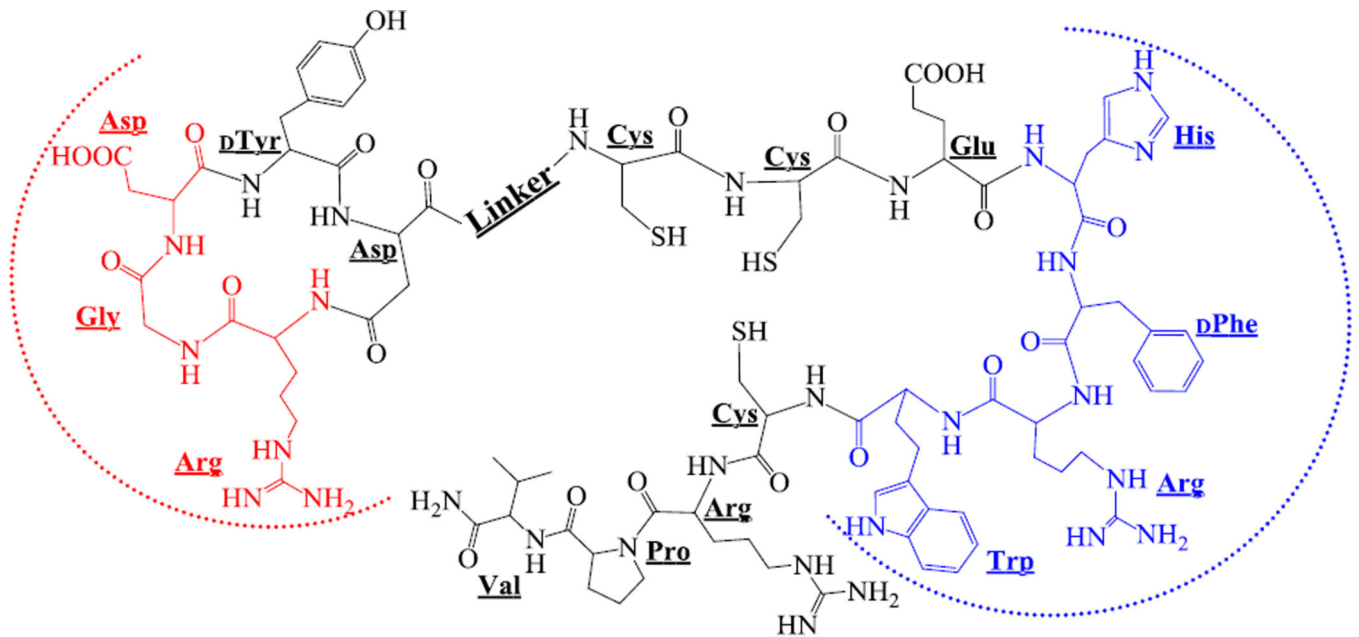
ACKNOWLEDGMENTS

REFERENCES

1. Giblin MF, Wang N, Hoffman TJ, Jurisson SS, Quinn TP. Design and characterization of alpha-melanotropin peptide analogs cyclized through rhenium and technetium metal coordination. Proc Natl Acad Sci USA. 1998; 95:12814–12818. [PubMed: 9788997]

2. Froidevaux S, Calame-Christe M, Tanner H, Sumanovski L, Eberle AN. A novel DOTA-alpha-melanocyte-stimulating hormone analog for metastatic melanoma diagnosis. J Nucl Med. 2002; 43:1699–1706. [PubMed: 12468522]

3. Miao Y, Benwell K, Quinn TP. ^{99m}Tc- and ^{111}In-labeled alpha-melanocyte-stimulating hormone peptides as imaging probes for primary and pulmonary metastatic melanoma detection. J Nucl Med. 2007; 48:73–80. [PubMed: 17204701]

4. Froidevaux S, Calame-Christe M, Schuhmacher J, Tanner H, Saffrich R, Henze M, et al. A gallium-labeled DOTA-alpha-melanocyte- stimulating hormone analog for PET imaging of melanoma metastases. J Nucl Med. 2004; 45:116–123. [PubMed: 14734683]

5. Miao Y, Figueroa SD, Fisher DR, Moore HA, Testa RF, Hoffman TJ, et al. ^{203}Pb-labeled alpha-melanocyte-stimulating hormone peptide as an imaging probe for melanoma detection. J Nucl Med. 2008; 49:823–829. [PubMed: 18413404]

6. Miao Y, Gallazzi F, Guo H, Quinn TP. ^{111}In-labeled lactam bridge-cyclized alpha-melanocyte stimulating hormone peptide analogues for melanoma imaging. Bioconjugate Chem. 2008; 19:539–547.

7. Guo H, Shenoy N, Gershman BM, Yang J, Sklar LA, Miao Y. Metastatic melanoma imaging with an ^{111}In-labeled lactam bridge-cyclized alpha-melanocyte-stimulating hormone peptide. Nucl Med Biol. 2009; 36:267–276. [PubMed: 19324272]

8. Cheng Z, Xiong Z, Subbarayan M, Chen X, Gambhir SS. ^{64}Cu-labeled alpha-melanocyte-stimulating hormone analog for MicroPET imaging of melanocortin 1 receptor expression. Bioconjugate Chem. 2007; 18:765–772.

9. Guo H, Yang J, Gallazzi F, Miao Y. Reduction of the ring size of radiolabeled lactam bridge-cyclized alpha-MSH peptide resulting in enhanced melanoma uptake. J Nucl Med. 2010; 51:418–426. [PubMed: 20150256]

10. Guo H, Yang J, Gallazzi F, Miao Y. Effects of the amino acid linkers on melanoma-targeting and pharmacokinetic properties of Indium-111-labeled lactam bridge-cyclized α-MSH peptides. J Nucl Med. 2011; 52:608–616. [PubMed: 21421725]

11. Guo H, Miao Y. Cu-64-labeled lactam bridge-cyclized α-MSH peptides for PET imaging of melanoma. Mol Pharm. 2012; 9:2322–2330. [PubMed: 22780870]

12. Cheresh DA, Spiro RC. Biosynthetic and functional properties of an Arg-Gly-Asp-directed receptor involved in human melanoma cell attachment to vitronectin, fibrinogen, and von Willebrand factor. J Biol Chem. 1987; 262:17703–17711. [PubMed: 2447074]

13. Cheresh DA, Harper JR. Arg-Gly-Asp recognition by a cell adhesion receptor requires its 130-kDa alpha subunit. J Biol Chem. 1987; 262:1434–1437. [PubMed: 2433281]

14. Albelda SM, Mette SA, Elder DE, Stewart R, Damjanovich L, Herlyn M, et al. Integrin distribution in malignant melanoma: association of the β3 subunit with tumor progression. Cancer Res. 1990; 50:6757–6764. [PubMed: 2208139]

15. Haubner R, Wester HJ, Reuning U, Senekowitsch-Schmidtke R, Diefenbach B, Kessler H, et al. Radiolabeled alpha(v)beta(3) integrin antagonists: a new class of tracers for tumor targeting. J Nucl Med. 1999; 40:1061–1071. [PubMed: 10452325]

16. Poethko T, Schottelius M, Thumshirn G, Hersel U, Herz M, Henriksen G, et al. Two-step methodology for high-yield routine radiohalogenation of peptides: ^{18}F-labeled RGD and octreotide analogs. J Nucl Med. 2004; 45:892–902. [PubMed: 15136641]

17. Yang J, Guo H, Miao Y. Technetium-99m-labeled Arg-Gly-Asp-conjugated alpha-melanocyte stimulating hormone hybrid peptides for human melanoma imaging. Nucl Med Biol. 2010; 37:873–883. [PubMed: 21055617]

18. Yang J, Guo H, Padilla RS, Berwick M, Miao Y. Replacement of the Lys linker with an Arg linker resulting in improved melanoma uptake and reduced renal uptake of Tc-99m-labeled Arg-Gly-

Asp-conjugated alpha-melanocyte stimulating hormone hybrid peptide. Bioorg Med Chem. 2010; 18:6695–6700. [PubMed: 20728365]

19. Hoffman TJ, Gali H, Smith CJ, Sieckman GL, Hayes DL, Owen NK, et al. Novel series of ^{111}In-labeled bombesin analogs as potential radiopharmaceuticals for specific targeting of gastrin-releasing peptide receptors expressed on human prostate cancer cells. J Nucl Med. 2003; 44:823–831. [PubMed: 12732685]

20. Smith CJ, Gali H, Sieckman GL, Higginbotham C, Volkert WA, Hoffman TJ. Radiochemical investigations of ^{99m}Tc-N$_3$S-X-BBN[7–14]NH2: an in vitro/in vivo structure-activity relationship study where X=0-, 3-, 5-, 8- and 11-carbon tethering moieties. Bioconjug Chem. 2003; 14:93–102. [PubMed: 12526698]

21. Parry JJ, Kelly TS, Andrews R, Rogers BE. In vitro and in vivo evaluation of ^{64}Cu-labeled DOTA-Linker-Bombesin(7–14) analogues containing different amino acid linker moieties. Bioconjug Chem. 2007; 18:1110–1117. [PubMed: 17503761]

22. Miao Y, Owen NK, Whitener D, Gallazzi F, Hoffman TJ, Quinn TP. In vivo evaluation of ^{188}Re labeled alpha-melanocyte stimulating hormone peptide analogs for melanoma therapy. Int J Cancer. 2002; 101:480–487. [PubMed: 12216078]

Figure 1.
Schematic structures of RGD-Aoc-(Arg[11])CCMSH and RGD-PEG$_2$-(Arg[11])CCMSH hybrid peptides. The binding sequences for MC1 and $\alpha_v\beta_3$ integrin receptors were highlighted with blue and red dashed half circles, respectively.
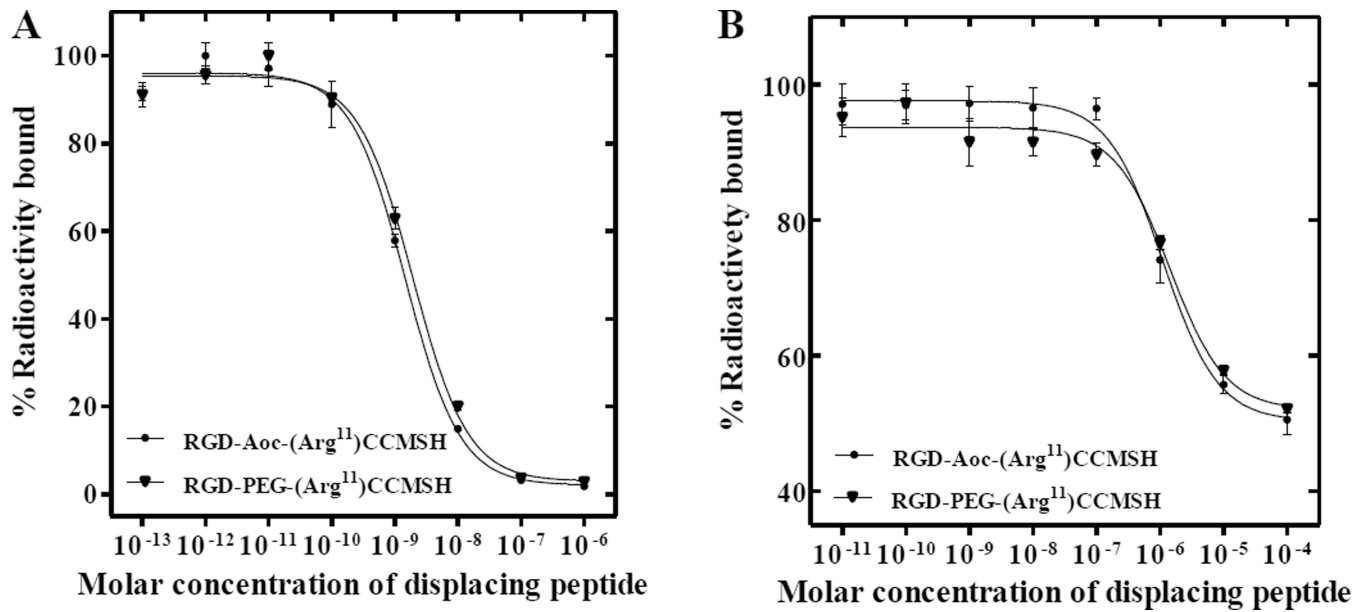
Figure 2.
The MC1 (A) and $\alpha_v\beta_3$ integrin (B) receptor competitive binding curves of RGD-Aoc-(Arg^{11})CCMSH and RGD-PEG$_2$-(Arg^{11})CCMSH hybrid peptides in M21 human melanoma cells. The IC$_{50}$ values of RGD-Aoc-(Arg^{11})CCMSH and RGD-PEG$_2$-(Arg^{11})CCMSH were 1.5 ± 0.2, 1.9 ± 0.2 nM for the MC1 receptor and 1125 ± 26, 1479 ± 74 nM for $\alpha_v\beta_3$ integrin receptor, respectively.
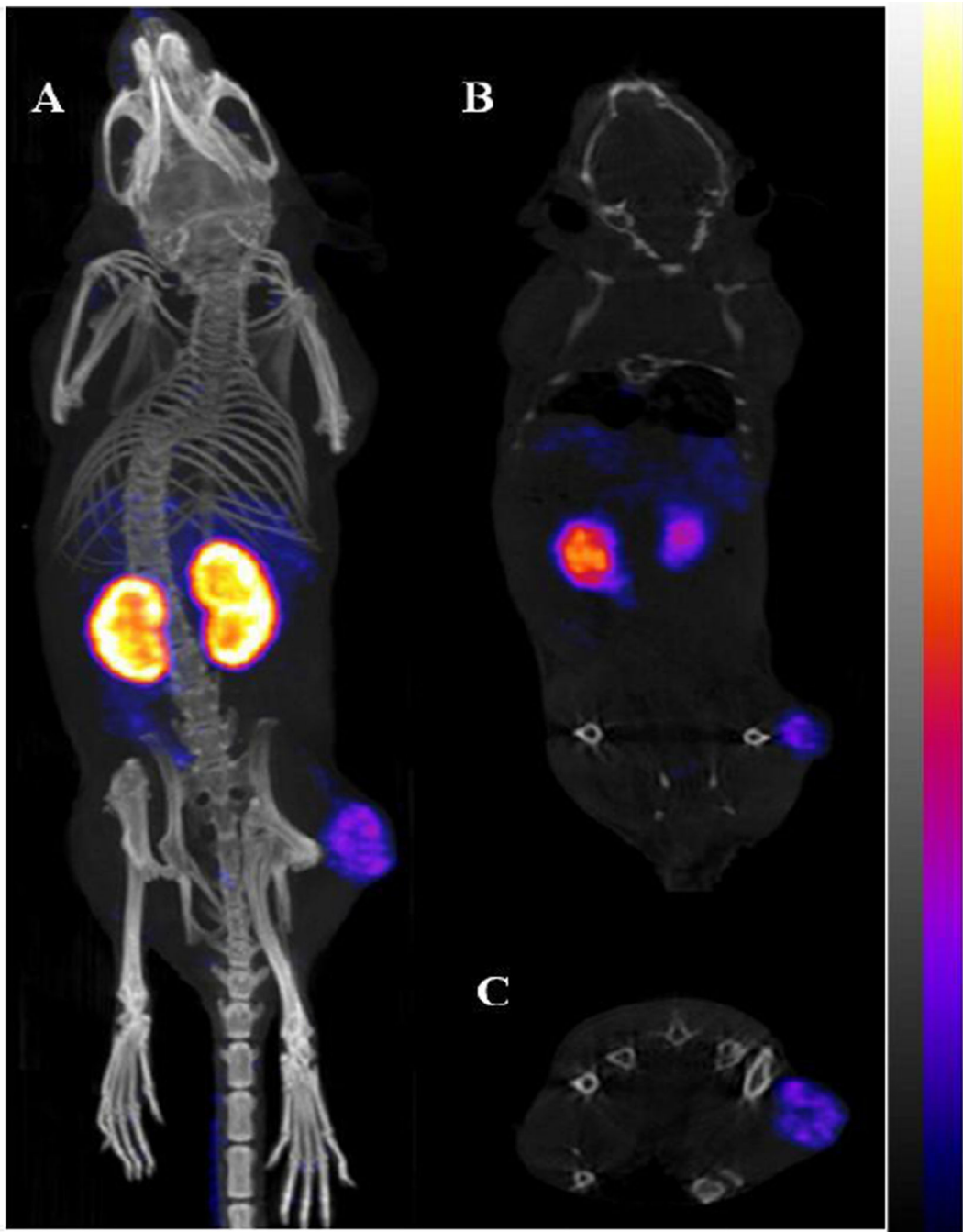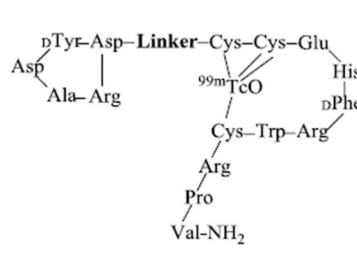
Figure 3.
Representative three-dimensional (A), coronal (B) and transversal (C) SPECT/CT images of M21 human melanoma xenografts at 2 h post-injection of 9.2 MBq of ^{99m}Tc-RGD-Aoc-(Arg^{11})CCMSH.
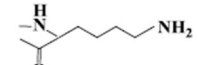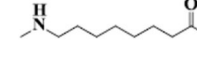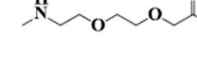
Peptide	Linker Structure	M21 melanoma uptake (%ID/g at 2 h PI)	Renal uptake (%ID/g at 2 h PI)
99mTc-RGD-Lys-(Arg11)CCMSH		2.69 ± 0.78	67.06 ± 16.53
99mTc-RGD-Aoc-(Arg11)CCMSH		2.35 ± 0.12	27.93 ± 3.98
99mTc-RGD-PEG2-(Arg11)CCMSH		1.71 ± 0.25	22.01 ± 9.89

Figure 4.
The melanoma and renal uptake of 99mTc-RGD-Linker-(Arg11)CCMSH peptides at 2 h post-injection in M21 human melanoma-xenografted nude mice. Data of 99mTc-RGD-Lys-(Arg11)CCMSH are cited for comparison [17].

Table 1

Biodistribution of ^{99m}Tc-RGD-Aoc-(Arg^{11})CCMSH (A) and ^{99m}Tc-RGD-PEG$_2$-(Arg^{11})CCMSH (B) in M21 h human melanoma-xenografted nude mice. The data was presented as percent injected dose/gram or as percent injected dose (mean ± SD, n = 5)

Tissue	A					B
	0.5 h	2 h	2 h blockade	4 h	24 h	2 h
	Percent injected dose/gram (%ID/g)					
Tumor	2.42 ± 0.23	2.35 ± 0.12	1.17 ± 0.15[b]	1.56 ± 0.26	0.64 ± 0.31	1.71 ± 0.25[c]
Brain	0.24 ± 0.04	0.11 ± 0.01	0.10 ± 0.01	0.07 ± 0.01	0.02 ± 0.01	0.02 ± 0.01
Blood	5.01 ± 0.47	1.90 ± 0.21	1.39 ± 0.28	1.54 ± 0.14	0.17 ± 0.03	1.52 ± 0.01
Heart	2.87 ± 0.17	1.28 ± 0.14	0.99 ± 0.13	1.04 ± 0.25	0.42 ± 0.12	0.20 ± 0.01
Lung	7.61 ± 1.05	3.85 ± 0.41	3.62 ± 0.49	2.73 ± 0.33	1.80 ± 0.10	0.79 ± 0.53
Liver	7.05 ± 0.91	4.69 ± 0.36	4.34 ± 0.61	4.82 ± 0.81	2.27 ± 0.61	1.12 ± 0.05
Skin	5.08 ± 0.46	2.20 ± 0.14	2.16 ± 0.31	1.90 ± 0.24	1.13 ± 0.28	1.16 ± 0.38
Spleen	2.83 ± 0.47	1.65 ± 0.25	1.25 ± 0.51	1.54 ± 0.23	1.37 ± 0.30	0.44 ± 0.27
Stomach	4.49 ± 0.38	4.98 ± 0.45	3.16 ± 0.16	4.78 ± 0.50	5.10 ± 0.87	0.66 ± 0.19
Kidneys	25.85 ± 9.14	27.93 ± 3.98	25.56 ± 3.30	37.05 ± 1.76	14.32 ± 2.37	22.01 ± 9.89
Muscle	1.01 ± 0.32	0.31 ± 0.13	0.32 ± 0.18	0.25 ± 0.02	0.14 ± 0.04	0.14 ± 0.16
Pancreas	0.90 ± 0.39	0.53 ± 0.13	0.28 ± 0.25	0.41 ± 0.14	0.21 ± 0.11	0.09 ± 0.04
Bone	1.55 ± 0.14	0.84 ± 0.16	0.66 ± 0.23	0.60 ± 0.10	0.30 ± 0.08	0.27 ± 0.09
	Percent injected dose (%ID)					
Intestines	4.22 ± 0.51	4.44 ± 0.55	3.49 ± 0.39	5.67 ± 0.16	4.68 ± 0.41	1.66 ± 0.37
Bladder	41.20 ± 8.69	59.87 ± 4.41	64.58 ± 5.43	63.71 ± 3.84	80.55 ± 6.26	81.36 ± 1.72
	Uptake ratio of tumor/normal tissue					
Tumor/Blood	0.48 ± 0.08	1.24 ± 0.09	0.84 ± 0.12	1.01 ± 0.18	3.76 ± 1.24	1.13 ± 0.08
Tumor/Kidneys	0.09 ± 0.04	0.08 ± 0.01	0.05 ± 0.01	0.04 ± 0.01	0.04 ± 0.02	0.08 ± 0.01
Tumor/Lung	0.32 ± 0.07	0.62 ± 0.07	0.32 ± 0.08	0.57 ± 0.09	0.36 ± 0.17	2.16 ± 1.43
Tumor/Liver	0.34 ± 0.05	0.50 ± 0.03	0.27 ± 0.04	0.32 ± 0.07	0.28 ± 0.17	1.53 ± 0.14
Tumor/Muscle	2.40 ± 0.91	7.58 ± 3.79	3.70 ± 1.31	6.12 ± 0.70	4.75 ± 2.20	12.21 ± 7.85

[b]
p<0.05, significance comparisons on tumor and renal uptake between ^{99m}Tc-RGD-Aoc-(Arg^{11})CCMSH (A) with/without peptide blockade at 2 h post-injection.

[c] $p<0.05$, significance comparisons on tumor and renal uptake between ^{99m}Tc-RGD-Aoc-(Arg^{11})CCMSH (A) and ^{99m}Tc-RGD-PEG$_2$-(Arg^{11})CCMSH (B) at 2 h post-injection.